



# Light trapping gratings for solar cells: an analytical period optimization approach

BENEDIKT BLÄSI,<sup>1,3</sup>  MARIO HANSER,<sup>1</sup> KLAUS JÄGER,<sup>2,4</sup>  AND OLIVER HÖHN<sup>1</sup> 

<sup>1</sup>Fraunhofer Institute for Solar Energy Systems, ISE, Heidenhofstraße 2, 79100 Freiburg, Germany

<sup>2</sup>Helmholtz-Zentrum Berlin für Materialien und Energie, Department Optics for Solar Energy, Albert-Einstein-Straße 16, 12489 Berlin, Germany

<sup>3</sup>benedikt.blaesi@ise.fraunhofer.de

<sup>4</sup>klaus.jaeger@helmholtz-berlin.de

**Abstract:** Solar cells can harvest incident sunlight very efficiently by utilizing grating-based light trapping. As the working principle of such gratings strongly depends on the number as well as the propagation directions of the diffraction orders, the grating period is a key parameter. We present an analytical model for optimizing the grating period, focusing on its impact on light path enhancement and outcoupling probability. Based on the presented model, we formulate guidelines to maximize light trapping in state-of-the-art high-end solar cells. The model increases the understanding of the grating performance in systems like the III-V//Si triple junction solar cell achieving record efficiency.

© 2022 Optica Publishing Group under the terms of the [Optica Open Access Publishing Agreement](#)

## 1. Introduction

Photovoltaic solar cells convert radiant energy from the sun into electrical energy. For a maximal power conversion efficiency (PCE), the fraction of the incident sunlight that is absorbed in the absorber layer of the solar cell must be maximized. Measures to increase the absorbed fraction of sunlight are usually termed *light management*.

Light management comprises mainly of two categories: First, *light in-coupling*, which includes all approaches to minimize reflective losses at the front, such as anti-reflective coatings or textured interfaces. Second, for some absorber materials the penetration depth is much longer than the absorber thickness in certain spectral regions of the incident sunlight. This means that only a small fraction of the light reaching the absorber really can be absorbed. For example, silicon with thickness  $> 100 \mu\text{m}$  absorbs weakly at wavelengths in proximity to its bandgap (appr. 1000–1200 nm) because its bandgap is indirect. For such materials, *light trapping* techniques are used to increase the absorption. In simple terms this is done by “prolonging the average path length” of the photons through the absorber, often by scattering at textured interfaces at one or both sides of the solar cell.

In the 1980s, Yablonovitch together with Tiedje showed that the absorption in a weakly absorbing layer can be enhanced up to a factor  $4n^2$  when scattering layers are implemented that randomize the light *ergodically* [1,2]. Miñano showed that the enhancement can reach an even higher factor of  $4n^2/\sin^2\theta$ , if the angular acceptance of the cell is restricted to a cone with opening angle  $\theta$  [3].

In conventional silicon solar cells, silicon wafers are textured with randomly distributed pyramids, which are created during anisotropic wet-chemical etching processes. This approach has been followed at least since 1974 [4] and is still applied in the current champion silicon solar cell with 26.7% PCE (as of February 2022) [5,6].

Besides texturization schemes with random features, also periodic texturing has been investigated for decades, for example for thin-film solar cells. In a carefully designed study Battaglia *et al.* prepared thin-film silicon solar cells with periodic and random nanotextures with comparable

geometrical dimensions and showed that the two devices performed similarly [7]. Bozzola and coworkers optimized one- and two-dimensional gratings for thin-film silicon solar cells and obtained designs, which approach the Lambertian limit for a large wavelength range [8]. Isabella *et al.* presented a thin-film silicon solar cell with pyramidal gratings on front and back sides with decoupled periods. These cells exceed Green's limit, a generalized version of the  $4n^2$  limit, for a large spectral range [9].

In the following paragraphs, we look at works on solar cells with optically thick absorbers, where waveguide effects can be neglected. In 1989 Kiess and Morf demonstrated experimentally that rectangular gratings in aluminum at the back of a silicon wafer increase the absorption [10]. In 1995, Heine and Morf designed blazed sub-micrometer gratings for solar cells such that reflection of light into the zeroth order is suppressed [11]. In 2011, Gjessing, Sudbø and Marstein found that a 'zig-zag' grating, which can be seen as an overlay of two blazed gratings which are rotated by  $90^\circ$  with respect to each other. This outperforms other two-dimensional designs [12], which corroborates the findings of Heine and Morf. The relevance of grating-based light trapping could recently be shown by the current champion III-V-on-silicon triple-junction solar cell with 35.9% PCE, featuring a crossed grating with period  $1\ \mu\text{m}$  at the rear of the silicon bottom cell [13,14].

Over the years, many different geometries for periodic gratings have been investigated and various optimization criteria have been applied. They use different design criteria, for example maximizing the coupling to diffraction orders that propagate at high angles within the cell and suppressing reflection into the  $0^{\text{th}}$  order [11,15], or by maximizing the diffraction efficiency into trapped orders [12,16]. Other studies use agnostic parameter scans [17,18] or optimization methods such as the Bayesian optimization method to further enhance the absorption in the silicon subcell by improving the geometry of the cross grating [19].

The different grating geometries make it difficult to extract the influence of the grating period, which probably is the most significant parameter to characterize a grating as it governs the propagation angles and thus significantly affects the light path enhancement and the outcoupling probability. Still, part of the grating periods identified as beneficial in silicon based solar cells can be categorized into two groups: (1) Periods between 300 nm and 350 nm, leading to first diffraction orders propagating almost parallel to the substrate, e.g. [10,17]. (2) Periods around 1000 nm, maximizing the number of trapped orders while avoiding higher orders in the escape cone, e.g. [12,14,17,18]. These two groups do not cover all of the results as some of the optimized grating structures have periods in between these values, thus forming a third group at about 700nm [11,19].

An analysis focused on the grating period was done by Yu, Raman and Fan, who showed in 2010 that periodic textures can enhance absorption more than  $4n^2$  in certain spectral and angular regions [20]. For that work they developed a statistical temporal coupled-mode theory of light trapping based on a rigorous electromagnetic approach, which works for thin layers.

In this work, we investigate the fundamental influence of the grating period for light trapping in optically thick solar cells. First, we develop a simple formalism to estimate the *light-path enhancement* (LPE) caused by crossed and hexagonal gratings at the back of non-absorptive bulk layers, where the period is the only parameter used to describe our gratings. Even though the model is based on very different assumptions than the theory developed by Yu, Raman and Fan, we show that both approaches lead to identical results for the LPE. Expanding the formalism to absorbing materials, we investigate the dependence of beneficial period ranges on cell thickness and parasitic absorptance. Furthermore, we compare the predictions of our model to a recent rigorous optimization study and experimental results. The model developed and discussed in this work deepens our insight into the key design parameters for periodic gratings and allows us to formulate guidelines for maximizing light trapping in state-of-the-art high-end solar cells. Here, we restrict ourselves to two-dimensional gratings, because they occupy larger fractions of

the optical phase space than one-dimensional gratings, which corresponds to a larger light-path enhancement [21].

## 2. Light trapping – the fundamentals

For a very basic light trapping model, the limiting case without absorption in the system is investigated. The key figure then is the Light Path Enhancement (LPE) factor in the system, which is defined as the length of the enhanced light path divided by the thickness of the solar cell. In the basic model, the LPE is calculated using two main ingredients: Firstly, the primary light path enhancement  $L_0$ , defined as the mean path length  $\ell_0$  light travels until the first outcoupling possibility divided by the wafer thickness  $w$ ,  $L_0 = \ell_0/w$ . Secondly the escape probability  $P_{\text{out}}$  at every interface with outcoupling possibility. The LPE can be calculated as a geometric series [22,23] resulting in

$$\text{LPE} = \frac{L_0}{P_{\text{out}}}. \quad (1)$$

For the well-known Lambertian case with ideal rear side reflector,  $L_0 = 2 \cdot 2 = 4$ . Here, one factor comes from the rear-side reflection (double pass) and the other factor from the average path enhancement caused by the scattering. If the front interface is perfectly transmitting apart from total internal reflection,  $P_{\text{out}} = 1/n^2$ , with the refractive index  $n$ . Consequently, we obtain the “Lambertian limit”  $4n^2$  [1] for the LPE. It is worth noting that for typical refractive indices of inorganic semiconductors, e.g.  $n \approx 3.5$  for silicon at wavelengths close to the band edge, the contribution of  $P_{\text{out}}$  to the LPE (12.25) is much larger than that of  $L_0$ . This indicates that  $P_{\text{out}}$  has a major impact on light trapping, as was also observed by Yablonovitch [24]. In the following, we will investigate this relation for diffraction gratings.

## 3. Modeling the impact of the grating period in the weakly absorbing limit

For understanding the influence of the grating period in grating based light trapping, we first perform an LPE analysis of an absorption free system using a basic model. Afterwards we evaluate the photocurrent density of absorbing systems, also including parasitic absorption.

For all the models, the following definitions and assumptions apply:

1. The investigated solar cell is optically thick. Hence, no wave-optical interactions (interference or wave-guide effects) between front and rear interface are considered.
2. The front interface is perfectly transmitting apart from total internal reflection ( $T = 1$  for incidence angles smaller than the critical angle).
3. The rear interface consists of a 100% reflective grating.
4. The solar cell is surrounded by air ( $n = 1.0$ ).
5.  $L_0$  is calculated from the polar diffraction angles using the term  $1/\cos \theta$ , averaged over all diffraction orders and multiplied by 2 (double pass).
6. We assume an equal intensity distribution over all diffraction orders (all diffraction efficiencies have the same value). This choice for achieving excellent light trapping is motivated by the following consideration: Miñano [3] states that the thermodynamic upper limit for light trapping is achieved if all trapped orders are illuminated with maximum brightness. If all diffraction efficiencies have the same value, the outcoupling probability is minimized (due to reciprocity), and high brightness in all trapped orders is achieved very efficiently. The assumption of equal distribution implies a requirement for the unit cell, which must be designed such that equal coupling efficiencies are ensured. Of course,

this choice limits the applicability of the findings. For example, the results are not valid for systems, which do not couple into certain diffraction orders (e.g. Reference [16])

7.  $P_{\text{out}}$  is calculated as the intensity in the outcoupling orders divided by the overall intensity impinging on the front surface from inside the cell.
8. The grating period  $\Lambda$  is defined as the length of the lattice vectors that span the unit cell. The lattice-plane distance  $d$  is the distance between adjacent lattice planes. For crossed gratings,  $d = \Lambda$ , while for hexagonal gratings  $d = \sqrt{3}/2 \cdot \Lambda$  (Fig. 1). Since the lattice-plane distance mainly governs the diffraction effects,  $d$  is used as key parameter throughout this manuscript. Since  $d$  and  $\Lambda$  are directly related, we still use the term *period* in headings and text for simplicity.

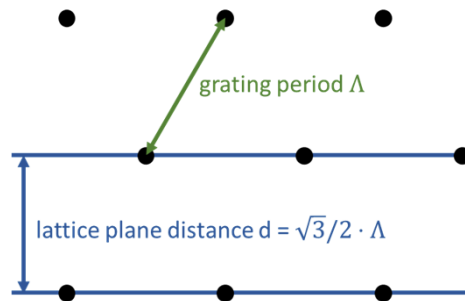


**Fig. 1.** Definition of period  $\Lambda$  and lattice plane distance  $d$  for the hexagonal grating.

### 3.1. Simple (statistical) way to calculate $L_0$ and $P_{\text{out}}$

To demonstrate the major influence of the grating period, we apply a basic statistical model, assuming no absorption in the system. The refractive index of the substrate is assumed as  $n = 3.5$ , which is very close to the value for silicon in the wavelength range 1000–1200 nm. Based on the equal distribution of diffraction efficiencies,  $P_{\text{out}}$  is then given as the relation of the number of diffraction orders in the escape cone divided by the total number of diffraction orders propagating in the bulk material.

In a first step,  $L_0$  and  $P_{\text{out}}$  are not calculated as exact values but as statistical values:

We assume  $L_0 = 2 \cdot 2$  as in Lambertian case. This is a good approximation for large  $d/\lambda$ , but will be inaccurate for small lattice plane distances.

While for the calculation of  $P_{\text{out}}$  the accurate number of escape modes is taken, the number of all modes is statistically calculated from the area of the  $k_{xy}$  space representing propagating waves in the bulk material divided by the area of the 1<sup>st</sup> Brillouin zone:

$$\text{area of the } k_{xy} \text{ space in bulk} = \pi \left( \frac{2\pi n}{\lambda} \right)^2 \quad (2)$$

$$\begin{aligned} \text{area of 1}^{\text{st}} \text{ Brillouin zone} \\ \text{(crossed grating)} \end{aligned} = \left( \frac{2\pi}{d} \right)^2 \quad (3)$$

$$\begin{aligned} \text{area of 1}^{\text{st}} \text{ Brillouin zone} \\ \text{(hexagonal grating)} \end{aligned} = \frac{\sqrt{3}}{2} \left( \frac{2\pi}{d} \right)^2 \quad (4)$$

The resulting formulae for the LPE are:

$$\text{LPE (crossed)} = \frac{4}{P_{\text{out,crossed}}} = \frac{4\pi n^2 \left(\frac{d}{\lambda}\right)^2}{M_{\text{esc}}} \quad (5)$$

$$\text{LPE (hexagonal)} = \frac{4}{P_{\text{out,hexagonal}}} = \frac{4\pi n^2 \frac{2}{\sqrt{3}} \left(\frac{d}{\lambda}\right)^2}{M_{\text{esc}}} \quad (6)$$

with the number of escape modes  $M_{\text{esc}}$

In Fig. 2 the LPEs for the crossed and hexagonal gratings are displayed. It is interesting to note that these equations, which we obtained from very simple assumptions, lead to exactly the same relationships as Yu *et al.* [20] derived them for multi-resonant light trapping in weakly absorbing waveguides.

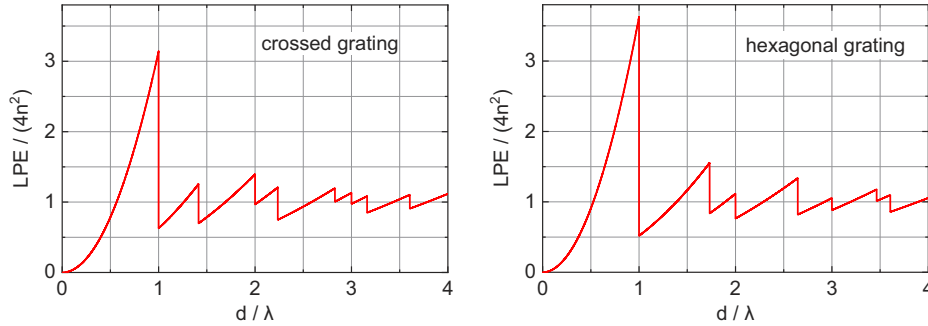


**Fig. 2.** LPE calculated with the basic model for the crossed and hexagonal grating. Note that this exactly agrees with the results from Yu *et al* [20].

Again, it is important to note that this basic model relies on many simplifications, resulting in limited validity for small values of  $d/\lambda$ . However, the strong impact of the grating period on mode ratio and outcoupling probability can already be seen with this formalism. So, we get a first indication that there is a beneficial parameter range for  $d/\lambda$  just below 1 when several diffraction orders can propagate in the substrate, but only the zeroth order can escape.

### 3.2. Improved model to understand the impact of the grating period

Until now, we used a strongly simplified approach, which will be refined in the following. Here, we calculate the values  $L_0$  and  $P_{\text{out}}$  exactly, while we previously only estimated them with statistical quantities. Here, we account for the divergence of the solar radiation as conical illumination, leading to cones of diffracted light. To calculate  $L_0$ , we integrate  $1/\cos \vartheta$  over all illuminated angles in the substrate.  $P_{\text{out}}$  is calculated as the area fraction of diffraction orders within the loss cone divided by the total area of diffraction orders in  $k_{xy}$  space (see Fig. 3):

$$P_{\text{out}} = \frac{\iint_{\text{illuminated, escaping}} 1 \, dk_x \, dk_y}{\iint_{\text{illuminated, substrate}} 1 \, dk_x \, dk_y}. \quad (7)$$

The basic concept used for calculating light trapping by the grating for conical illumination can be found in [16,25]. Figure 4 shows  $L_0$ ,  $1/P_{\text{out}}$  and  $\text{LPE} = L_0/P_{\text{out}}$  for the crossed grating. From the  $L_0$  plot (Fig. 4 a), it can be seen that strong light path enhancement occurs at  $d/\lambda$  values corresponding to very high propagation angles. For very large  $d/\lambda$  values,  $L_0$  converges

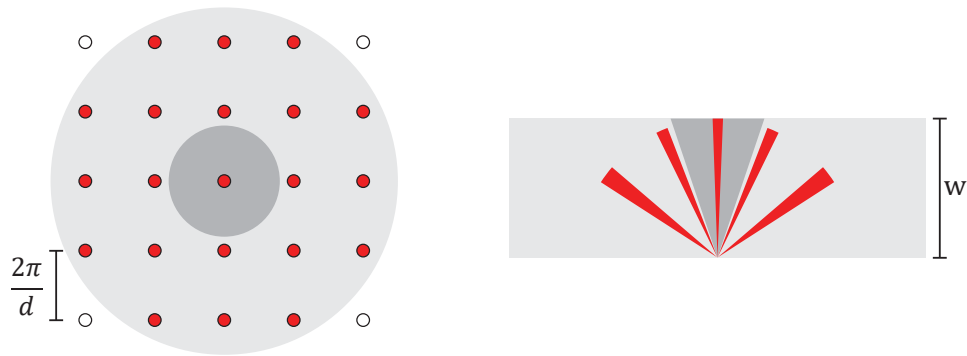


**Fig. 3.** Cones of diffracted light (red), represented in the  $k_{xy}$  space (left) and in real space (right). For the calculation of  $L_0$ ,  $1/\cos \theta$  is integrated over all red circles. For calculating  $P_{\text{out}}$ , the area of red circles within the dark grey area is divided by the area of all red circles.

to 2 as it approaches the Lambertian case (shown in the supplemental document, Fig. S2). The  $1/P_{\text{out}}$  plot (Fig. 4 b) shows a stepwise change of the outcoupling probability determined by the relation of modes (Eq. (7)). The largest step occurs at  $d/\lambda = 1$ , when the first higher orders enter the escape cone. For very large  $d/\lambda$  values,  $1/P_{\text{out}}$  converges to  $n^2 = 12.25$  as expected for the Lambertian case (see supplemental document). Since the LPE (Fig. 4 c) combines both parameters, both effects interact. Although very high and narrow peaks stand out, for a broadband application such as solar energy conversion no relevant impact from these peaks is to be expected. On the other hand, regions with high LPE values over a broader range of values are likely to lead to good light trapping. This can be seen for the approximate intervals  $0.64 < d/\lambda < 0.7$  and for  $0.81 < d/\lambda < 1$ . Similar observations can be made for the hexagonal case (shown in the supplemental document, Fig. S3 and S4).

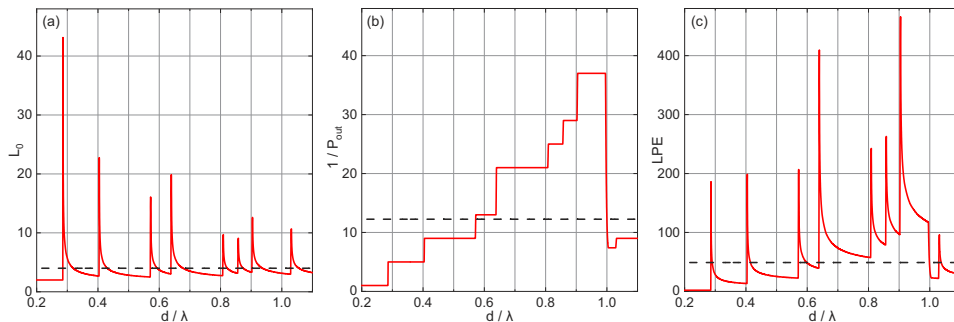


**Fig. 4.** Plots for  $L_0$ ,  $1/P_{\text{out}}$  and  $LPE = L_0/P_{\text{out}}$  for the crossed grating. As reference, the values for the Lambertian case are plotted as dashed line.

A comparison of the simple and the refined models is shown in Fig. 5. While the overall shape and the main outcoupling effects can already be seen from the simple model, the detailed impact of  $L_0$  and  $P_{\text{out}}$  on the LPE can only be identified in the plots based on the refined model. As expected, the difference between the models is strongest for small  $d/\lambda$  values.

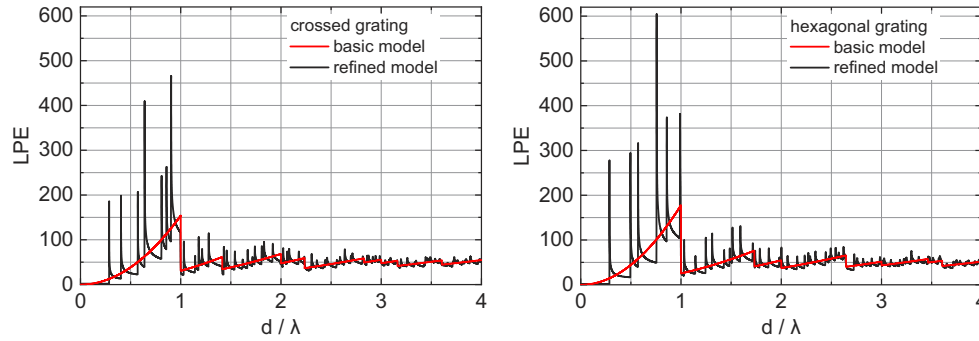


Fig. 5. comparison of simple and refined models for crossed and hexagonal grating.

#### 4. Modeling the impact of the grating period including absorption

For a more realistic assessment of light trapping in solar cells, we have to consider broadband illumination and the wavelength-dependent optical properties (refractive index and absorption) of the solar cell material. In this study, we focus on silicon using the optical data from Ref. [26]. To integrate the silicon absorption and parasitic rear-side absorption into the model, we extended Goetzberger's model for Lambertian light trapping [27] to systems with rear-side grating (details in the supplemental document, section S1). With this, the absorptance in the bulk  $A(\lambda)$  is

$$A(\lambda) = \frac{1 - I_0(\lambda)^2 P_{\text{out}}(\lambda) R_{\text{rear}}(\lambda) - I_0(\lambda)[1 - R_{\text{rear}}(\lambda)] - G(\lambda) R_{\text{rear}}(\lambda)}{1 - G(\lambda) R_{\text{rear}}(\lambda)} \quad (8)$$

With the fraction of intensity reaching the rear after the first (perpendicular) pass  $I_0$ , the rear side reflectance at every interaction  $R_{\text{rear}}$ , and the intensity for all trapped light paths arriving at the back side a second time  $G$ . In general, all these quantities are wavelength dependent. Furthermore,  $I_0$  and  $G$  depend on the cell thickness  $w$ .

Once absorption and broadband illumination are considered, path length enhancement is no meaningful parameter any longer since it strongly depends on absorption and wavelength. Therefore, we use the wavelength dependent absorptance to calculate the photocurrent density  $J_{\text{ph}}$ :

$$J_{\text{ph}} = q \int_{300 \text{ nm}}^{1200 \text{ nm}} \phi(\lambda)_{\text{AM1.5g}} \cdot A(\lambda) d\lambda \quad (9)$$

with the elementary charge  $q$  and the photon flux under AM1.5g illumination  $\phi(\lambda)_{\text{AM1.5g}}$  [28]. We set the default cell thickness to 280  $\mu\text{m}$  to make the results comparable with previous experimental and theoretical work [13,19]. For a cell of this thickness, the photocurrent density without light trapping and a perfect planar rear reflector would be 41.5  $\text{mA}/\text{cm}^2$ .

Figure 6 (left) shows the photocurrent density in dependence of the lattice plane distance  $d$  for both grating types. For comparison, the value that could be expected for a cell of the same thickness with Lambertian light trapping (calculated according to Ref. [29]) is shown as a dashed line. Beneficial ranges for  $d$  can be identified around 750 nm and between 930 nm and 1090 nm for the crossed grating and around 670 nm and between 860 nm and 1080 nm for the hexagonal grating. If one keeps in mind that for 280  $\mu\text{m}$  thick solar cells the biggest potential for light trapping is in the spectral range around 1100 nm, these values correspond well with the ranges identified as beneficial for the weakly absorbing limit. In Fig. 6 (right),  $J_{\text{ph}}$  is plotted for various cell thicknesses for the crossed grating. As expected, the absolute values decrease with decreasing cell thickness. However, the shape of the curves is very similar for all thicknesses. The shift of the peak positions towards smaller  $d$  values with decreasing thickness can be well

understood: For thinner cells the weakly absorbing spectral range for which light trapping is beneficial is extended towards smaller wavelengths. Therefore, gratings with a smaller  $d$  are most effective, since they also have an impact on smaller wavelengths. The same features can be observed for the hexagonal grating (supplemental document, Fig. S5).

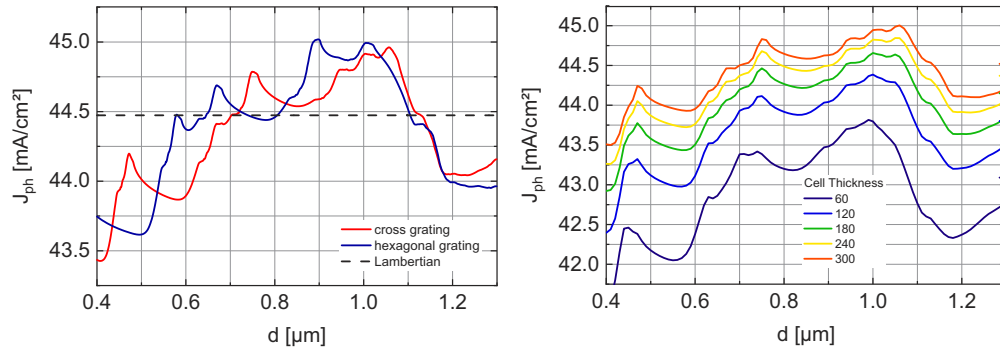


**Fig. 6.** Photocurrent density in dependence of the lattice plane distance  $d$  for the fixed cell thickness  $280 \mu\text{m}$  and both grating types (left) and for a thickness variation (crossed grating, right). The arrows at the right side indicate the photocurrent densities for Lambertian light trapping at the corresponding thicknesses.

Typically, introducing rear-side light trapping also implies a certain amount of parasitic absorption at the rear interface. In fact, balancing the light trapping performance and the parasitic absorption is key for achieving a good overall performance. Therefore, it is important to consider the impact of  $R_{\text{rear}}$  as well. To understand the main dependencies,  $R_{\text{rear}}$  is modeled as wavelength-independent quantity.

These interrelations are displayed in Fig. 7. For  $R_{\text{rear}} = 1$ , the values are the same as in Fig. 6 (left). With decreasing rear-side reflectance, gratings with smaller  $d$  get more favorable compared to larger lattice-plane distances. If one assumes  $R_{\text{rear}} \approx 0.95$  as a very high but realistic value, two peaks of similar height can be identified for the crossed grating:  $d = 0.75 \mu\text{m}$  and  $d = 1.0 \mu\text{m}$ . These two values correspond well with the periods that achieved peak values in the optimization by Tillmann *et al.* [19]. There,  $J_{\text{ph}}$  is maximal at  $d = 0.755 \mu\text{m}$ , while for lattice-plane distances just above  $1 \mu\text{m}$ , a second maximum can be seen. The results are also in accordance with the findings in Ref. [17] (with beneficial periods around  $0.73 \mu\text{m}$  and  $0.99 \mu\text{m}$ ) and [18] (beneficial period around  $1.08 \mu\text{m}$ ). Given that the investigated gratings and the used methods differ substantially, the convergence of the results confirms that our models are capable to reproduce fundamental trends. Furthermore, our findings match perfectly with the excellent light trapping performance of the crossed gratings with  $d = 1 \mu\text{m}$  which led to the record efficiencies of Si based triple junction solar cells [13,14].

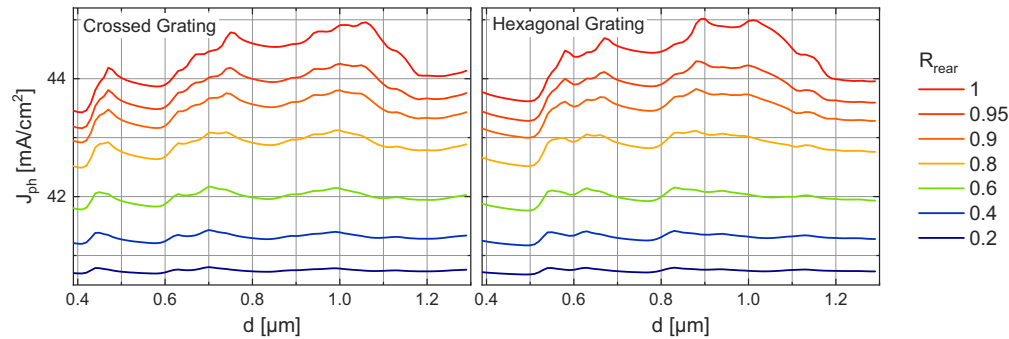


**Fig. 7.** Photocurrent density in dependence of the lattice plane distance  $d$  and the rear side reflectance  $R_{\text{rear}}$  for the fixed cell thickness  $280 \mu\text{m}$  for crossed gratings (left) and hexagonal gratings (right).

## 5. Interpretation and conclusions

The presented models demonstrate the impact of the grating period on the light trapping performance. The refined model introduced and discussed in sections 3.2 and 4 – which is a stark simplification with respect to realistic systems – accounts for many important parameters that influence the overall light trapping performance. Therefore, fundamental trends and interdependencies can be reproduced well, and strategies for the grating optimization can be derived. However, the model is not suitable for quantitative optimizations, because the absolute values cannot be expected to be accurate, and small differences e.g. between peak heights should be regarded as insignificant.

Based on our models the following conclusions can be drawn:

- For a good light trapping grating, the interplay of the primary light path enhancement  $L_0$  and the escape probability  $P_{\text{out}}$  is important. Both quantities need to be optimized together to achieve high LPE and photocurrent density  $J_{\text{ph}}$ .
- Small periods with very few propagating orders are not the best choice in most cases. They only might be beneficial in cases with high parasitic absorption.
- The identified sweet spots feature a larger number of propagating orders, moderate  $L_0$  enhancements and a low  $P_{\text{out}}$ .
- No significant difference in performance can be expected between crossed and hexagonal lattice symmetry.
- Keeping the parasitic absorption very low is crucial for achieving high  $J_{\text{ph}}$  values.

With these guidelines, gratings for high efficiency solar cells can be designed and used as starting points for further fine-tuning based on refined modelling and experimental evaluation. Due to the high  $J_{\text{ph}}$  level and the width of the peak, we recommend a crossed or hexagonal grating with a period close to  $1 \mu\text{m}$  for Si and III-V//Si solar cells. Furthermore, the presented models allow a basic understanding why certain grating designs work particularly well in simulations (e.g. [19]) or champion solar cells [13,14].

**Funding.** Bundesministerium für Wirtschaft und Energie (FKz. 0324247-PoTaSi); Fraunhofer-Gesellschaft (ICON project MEEt).

**Acknowledgments.** We would like to thank Andrea Cordaro and Albert Polman (AMOLF), Alexander Mellor (Naked Energy), Ralph Müller (Fraunhofer ISE) and Peter Tillmann (Helmholtz-Zentrum Berlin) for fruitful discussions.

**Disclosures.** The authors declare no conflicts of interest.

**Data availability.** Data underlying the results presented in this paper are not publicly available at this time but may be obtained from the authors upon reasonable request.

**Supplemental document.** See [Supplement 1](#) for supporting content.

## References

1. E. Yablonovitch, "Statistical ray optics," *J. Opt. Soc. Am.* **72**(7), 899–907 (1982).
2. T. Tiedje, E. Yablonovitch, G. D. Cody, and B. G. Brooks, "Limiting efficiency of silicon solar cells," *IEEE Trans. Electron Devices* **31**(5), 711–716 (1984).
3. J. C. Miñano, "Optical Confinement in Photovoltaics," in *Physical limitations to photovoltaic energy conversion*, A. Luque López and G. L. Araújo, eds. (Hilger, 1990), pp. 50–83.
4. J. G. Haynos, J. F. Allison, R. A. Arndt, and A. Meulenberg, "The COMSAT non-reflective silicon solar cell: a second generation improved cell," in *International Conference on Photovoltaic Power Generation* (1974), pp. 487–497.
5. K. Yoshikawa, H. Kawasaki, W. Yoshida, T. Irie, K. Konishi, K. Nakano, T. Uto, D. Adachi, M. Kanematsu, H. Uzu, and K. Yamamoto, "Silicon heterojunction solar cell with interdigitated back contacts for a photoconversion efficiency over 26%," *Nat. Energy* **2**(5), 17032 (2017).
6. M. A. Green, E. D. Dunlop, J. Hohl-Ebinger, M. Yoshita, N. Kopidakis, and X. Hao, "Solar cell efficiency tables (version 59)," *Prog Photovoltaics* **30**(1), 3–12 (2022).
7. C. Battaglia, C.-M. Hsu, K. Söderström, J. Escarré, F.-J. Haug, M. Charrière, M. Boccard, M. Despeisse, D. T. L. Alexander, M. Cantoni, Y. Cui, and C. Ballif, "Light trapping in solar cells. Can periodic beat random?" *ACS Nano* **6**(3), 2790–2797 (2012).
8. A. Bozzola, M. Liscidini, and L. C. Andreani, "Photonic light-trapping versus Lambertian limits in thin film silicon solar cells with 1D and 2D periodic patterns," *Opt. Express* **20**(S2), A224–A244 (2012).
9. O. Isabella, R. Vismara, D. Linssen, K. X. Wang, S. Fan, and M. Zeman, "Advanced light trapping scheme in decoupled front and rear textured thin-film silicon solar cells," *Sol. Energy* **162**, 344–356 (2018).
10. H. Kiess and R. Morf, "Light Trapping In Solar Cells And Determination Of The Absorbed Energy By Calorimetry," in *Optical Materials Technology for Energy Efficiency and Solar Energy Conversion VIII*, Vol. 1149 of Proceedings of SPIE (1989), pp. 124–129.
11. C. Heine and R. H. Morf, "Submicrometer gratings for solar energy applications," *Appl. Opt.* **34**(14), 2476–2482 (1995).
12. J. Gjessing, A. S. Sudbø, and E. S. Marstein, "Comparison of periodic light-trapping structures in thin crystalline silicon solar cells," *J. Appl. Phys.* **110**(3), 033104 (2011).
13. R. Cariou, J. Benick, F. Feldmann, O. Höhn, H. Hauser, P. Beutel, N. Razek, M. Wimplinger, B. Bläsi, D. Lackner, M. Hermle, G. Siefert, S. W. Glunz, A. W. Bett, and F. Dimroth, "III–V-on-silicon solar cells reaching 33% photoconversion efficiency in two-terminal configuration," *Nat. Energy* **3**(4), 326–333 (2018).
14. P. Schygulla, R. Müller, D. Lackner, O. Höhn, H. Hauser, B. Bläsi, F. Predan, J. Benick, M. Hermle, S. W. Glunz, and F. Dimroth, "Two-terminal III–V/Si triple-junction solar cell with power conversion efficiency of 35.9% at AM1.5g," *Prog Photovoltaics*, pip.3503 (2021).
15. C. E. A. Cordaro, N. Tucher, S. Tabernig, H. Hauser, O. Höhn, R. Müller, B. Bläsi, and A. Polman, "Plasmonic and Mie scattering in nanopatterned back reflectors for III–V-on-silicon solar cells (Conference Presentation)," in *Photonics for Solar Energy Systems VIII. 6-10 April 2020, online only, France, volume 11366 of Proceedings of SPIE* (SPIE, 2020), p. 6.
16. A. Mellor, I. Tobias, A. Marti, M. J. Mendes, and A. Luque, "Upper limits to absorption enhancement in thick solar cells using diffraction gratings," *Prog Photovoltaics* **19**(6), 676–687 (2011).
17. I. M. Peters, M. Rüdiger, H. Hauser, M. Hermle, and B. Bläsi, "Diffractive gratings for crystalline silicon solar cells—optimum parameters and loss mechanisms," *Prog. Photovolt: Res. Appl.* **20**(7), 862–873 (2012).
18. A. Mellor, I. Tobias, A. Marti, and A. Luque, "A numerical study of Bi-periodic binary diffraction gratings for solar cell applications," *Sol. Energy Mater. Sol. Cells* **95**(12), 3527–3535 (2011).
19. P. Tillmann, B. Bläsi, S. Burger, M. Hammerschmidt, O. Höhn, C. Becker, and K. Jäger, "Optimizing metal grating back reflectors for III-V-on-silicon multijunction solar cells," *Opt. Express* **29**(14), 22517 (2021).
20. Z. Yu, A. Raman, and S. Fan, "Fundamental limit of light trapping in grating structures," *Opt. Express* **18**(S3), A366 (2010).
21. I. M. Peters, "Phase space considerations for light path lengths in planar, isotropic absorbers," *Opt. Express* **22**(S3), A908–A920 (2014).
22. M. A. Green, *Silicon solar cells. Advanced principles & practice* (Centre for Photovoltaic Devices and Systems Univ. of New South Wales, 1995).
23. K. R. Catchpole and A. Polman, "Design principles for particle plasmon enhanced solar cells," *Appl. Phys. Lett.* **93**(19), 191113 (2008).
24. E. Yablonovitch and Yablonovitch, "Inhibited spontaneous emission in solid-state physics and electronics," *Phys. Rev. Lett.* **58**(20), 2059–2062 (1987).
25. I. Tobias, A. Luque, and A. Martí, "Light intensity enhancement by diffracting structures in solar cells," *J Appl Phys* **104**(3), 034502 (2008).

26. M. A. Green, "Self-consistent optical parameters of intrinsic silicon at 300 K including temperature coefficients," *Sol. Energy Mater. Sol. Cells* **92**(11), 1305–1310 (2008).
27. A. Goetzberger, "Optical confinement in thin Si-solar cells by diffuse back reflectors," in *Proceedings of the 15th IEEE Photovoltaic Specialists Conference* (1981), pp. 867–870.
28. ASTM G173-03, *Tables for Reference Solar Spectral Irradiances: Direct Normal and Hemispherical on 37 Tilted Surface*, 2012.
29. M. A. Green, "Lambertian light trapping in textured solar cells and light-emitting diodes. analytical solutions," *Prog Photovoltaics* **10**(4), 235–241 (2002).